Modulational instability of optically induced nematicon propagation

L. Kavitha[a)b)c)†], M. Venkatesh[a)], S. Dhamayanthi[a)], and D. Gopi[c)d)]

[a)] *Department of Physics, Periyar University, Salem-636 011, India*
[b)] *The Abdus Salam International Center for Theoretical Physics, Trieste, Italy*
[c)] *Center for Nanoscience and Nanotechnology, Periyar University, Salem-636 011, India*
[d)] *Department of Chemistry, Periyar University, Salem-636 011, India*

(Received 1 February 2013; revised manuscript received 30 May 2013)

We report the modulational instability (MI) analysis for the modulation equations governing the propagation of coherent polarized light through a nematic liquid crystal (NLC) slab, in the limit of low light intensity and local material response. The linear stability analysis of the nonlinear plane wave solutions is performed by considering both the wave vectors (k,l) of the basic states and wave vectors (K,L) of the perturbations as free parameters. We compute the MI gain, and the MI gain peak is reduced and the stable bandwidth is widened with the increase of the strength of the applied electric field. Further, we invoke the extended homogeneous balance method and Exp-function method aided with symbolic computation and obtain a series of periodic solitonic humps of nematicon profiles admitting the propagation of laser light in the NLC medium.

Keywords: solitons, computational methods, liquid crystals, nonlinearity

PACS: 94.05.Fg, 46.15.−x, 64.70.pp, 47.20.Ky **DOI:** 10.1088/1674-1056/22/12/129401

1. Introduction

Spatial solitary waves or solitons are known to occur in various fields including fluids, plasma, biology, matter wave, and optics.[1,2] They are often considered ubiquitous and share a number of fundamental properties relying on the combination of a nonlinear response and the natural tendency of a wave packet to spread as it propagates. Spatial solitons in optics are recognized as fundamental nonlinear electromagnetic wave objects with potential applications to all optical signal processing[3,4] and have been explored in several materials and configurations for signal readdressing.[5,6] Nematic liquid crystals (NLC) are unique materials, found in most consumer electronics applications. Research on the nonlinear optical properties of NLC has been limited to transverse effects in thin films. On many occasions, photorefractive NLC shows strong optical nonlinearity at much weaker laser powers. The electric field of an optical beam can change the orientation of the molecules in the nematic liquid crystal. In return, the material properties seen by the optical beam will change, in particular, the refractive index becomes intensity-dependent and this is an optical nonlinear effect denoted as optical field-induced director reorientation.[7–9] Although an optical beam focused in a liquid crystal layer will diffract with the increase in optical power, the self-focusing (or defocusing) of light occurs due to this nonlinear effect, depending on the geometry of NLC medium. When the self-focusing balances diffraction, the beam may propagate without change of its intensity profile, thus witnessing the formation of a spatial optical solitary wave packet.[10–12] Such soliton-like optical beam propagation was reported in nematic liquid crystals, with a few milliwatts of light power.[13] However, the major possible application concerns the dynamics of the soliton formation[14] and for applications in computing, optical interconnects may be useful to reduce the network latency due to a higher bandwidth of optical connections.[15] Indeed, adding reconfigurability to the optical interconnects can open new possibilities by enhancing the speed of the multiprocessor system, however, an adequate switching speed of the order of microsecond is required to outdo the electrical interconnects.[16] Also, for building an optical network the speed and the ease of switching light between fibers is of importance. Displays made with NLC typically have a refresh rate of a few tens of milliseconds[17] and we can expect that the soliton formation will be of the same order of magnitude.

Several reduced mathematical models for the optical switching process in a bulk NLC have been derived. Beginning from the most fundamental coupled field models of partial differential equations (PDE) that captures the essential coupling between optical refraction and nematic deformation,[18] self-focusing and filamentation mode is witnessed.[11] The model represents a two-dimensional (2D) spatial evolution of director reorientation governed by an evolution equation of the second order in space domain, requires the structure to be solved over a wide range of optical scales and poses considerable computational difficulty. In 1997, Snyder *et al.*, theoretically investigated solitons in a highly nonlocal medium, proposing a power-dependent parabolic refractive index profile.[19] The propagation of light in LCs with a local response has been considered by Khoo in several contexts.[8]

†Corresponding author. E-mail: louiskavitha@yahoo.co.in

© 2013 Chinese Physical Society and IOP Publishing Ltd

In particular, the nonlinear Schrödinger equation, which is valid for the nonlocal response of a medium, has been derived for LCs.[20] Also, equations for stimulated orientational scattering in LC with local response have been derived by Sarkissian *et al.*[21] Finally, the theoretical existence of nematicons in LCs has been pointed out by Conti *et al.*, and these nematicons are denoted as T solitons.[13]

This paper is organized as follows. In Section 2, we describe the formulation of the model. We perform linear stability analysis and derive the conditions for modulational instability in Section 3. Section 4 is devoted to the explicit derivation of a series of solutions by invoking the extended homogeneous balance (HB) method and Exp-function method. Further, we compare the solutions obtained by both methods. Section 5 concludes the paper.

2. Formulation of nematicon equations

In liquid crystal materials, the origin of locality is known: it is linked to the reorientational process, which itself is ruled by the elasticity of these materials. The optically induced index gradient is the result of the balance between the optically induced torque and the elastic torque generated by LC boundary conditions. However, the elastic forces between the liquid crystal molecules act as a diffusion mechanism[8] and the equilibrium on the whole LC system occurs on a large timescale depending on its thickness. This can be explained by comparing the time and spatial derivatives in the Euler–Lagrange equation, which rules out the optically induced reorientation.[22] Reinbert *et al.* investigated the propagation of nematicons in an NLC with a Kerr-type medium of a low power input optical field using a nonlinear Schrödinger (NLS) equation modified by a higher nonlinearity. The dynamical equation for the evolution of a nematicon/spatial soliton, which included the effect of shed dispersive radiation, was derived and its solutions are found to be in good agreement with full numerical solutions of the governing nematicon equation.[23,24] Conti *et al.* studied the solitary wave solutions of this NLS equation denoted by T-soliton solutions.[13] In this paper, we consider the same model of modulation equation which represents the interaction of light with the nematic system and investigate the modulational instability analysis to locate the domain of the stability/instability of the nematicons.

In this paper, we consider the same modulation equations for the evolution of a nematicon in a liquid crystal proposed by Reinbert *et al.*[23] We consider the propagation of coherent polarized light through a nematic liquid crystal slab.[24] The basic configuration is shown in Fig. 1. For this, we assume that our liquid crystal system is contained in an extremely narrow container with homeotropic alignment of molecules and with strong surface anchoring at the boundaries. A static electric field is applied parallel to the x axis in order to pretilt the nematic except near boundaries. A typical distribution of the pretilt angle ϕ is designated as shown in Fig. 1. The nematicon is then taken to propagate in the z direction and the axes are oriented such that the z axis is the direction of propagation of light. We denote that the director angle ϕ of the nematic molecule is measured from the z axis in the x–z plane and it is the angle that the optic axis makes with the propagation direction z. The equations for the electric field of the input polarized light $\boldsymbol{E}$ and the optical director angle ϕ is given by

$$\mathrm{i}\frac{\partial E}{\partial z}+\frac{1}{2}\nabla^2 E-\cos(2\phi)E=0, \tag{1}$$

$$\nu\nabla^2\phi-q\sin(2\phi)+2|E|^2\cos(2\phi)=0. \tag{2}$$

Equation (1) satisfies the Foch–Leontovich equation for the slowly varying envelope E of the electric field as given by Conti *et al.*,[13] and Assanto *et al.*[25] Equation (2) for the optic axis ϕ is obtained from the extremization of the free energy of the nematic which is given by Conti *et al.* The parameter q is related to the strength of the external static electric field. The parameter ν represents the strength of the nonlocality, which is the ratio of the elastic energy of the nematicon to the energy of the electric field. In the limit of local material response $\nu\to 0$, the director equation (2) can be approximated by the algebraic equation

$$-q\sin(2\phi)+2|E|^2\cos(2\phi)=0, \tag{3}$$

which has the solution

$$\tan(2\phi)=\frac{2|E|^2}{q}. \tag{4}$$

The initial condition at $z=0$ is taken to be a soliton-like pulse of the form

$$E(0,r)=A\mathrm{sech}\frac{r}{w}. \tag{5}$$

For a small amplitude A and for a large q, the modulation equations yield the following higher order nonlinear Schrödinger equation

$$\mathrm{i}\frac{\partial E}{\partial z}+\frac{1}{2}\nabla^2 E+\frac{2}{q}|E|^2E-\frac{4}{q^3}|E|^6E=0. \tag{6}$$

Further, we attempt to perform the modulational instability analysis and construct a series of exact propagating nematicon profiles.

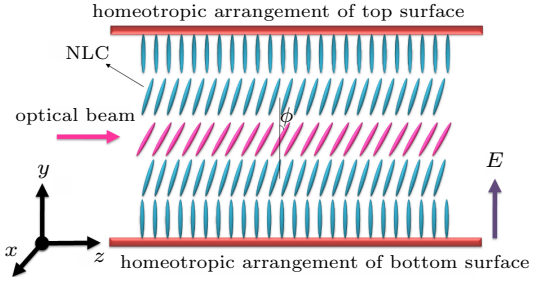


Fig. 1. (color online) Schematic diagram of nematic liquid crystal system with the propagation of polarized light along z direction.

3. Modulational instability analysis

The study of the dynamics of nonlinear waves is central to understand the behavior of a wide range of physical systems.[26–32] In recent years, an important theme of much of this work has been the study of modulational instabilities of plane waves. The use of nonlinear envelope (or amplitude) equations for studying the stability of patterns is widely employed. Our interest is the modulational instability (MI) of the slowly varying envelope E of the electric field in a set of modulation equations for the evolution of nematicon in a liquid crystal. MI is the outcome of interplay between nonlinear and dispersion effects. MI is a symmetry-breaking instability so that a small perturbation on top of a constant amplitude background experiences experimental growth and leads to the breakup of the spatial-temporal profile of a wave into a train of ultrashort pulses. MI analysis is usually carried out by means of the following scheme. First, one finds an equilibrium state of the system (6), which admits a family of traveling wave solutions. Second, one adds a small perturbation on the equilibrium state with a perturbation wave number and frequency, which are much smaller than those of the carrier wave. The small perturbation functions satisfy a set of equations from which the nonlinear dispersion relation is deduced. The later is analyzed to obtain a complex frequency, revealing the growth of the amplitude-modulated wave. Based on the above idea, one finds that the conditions under which a uniform wave train moving along the nematic will become stable, or unstable under small perturbations.

We begin our analysis on the stability by considering an exact continuous wave solution of Eq. (6) in the form

$$E = A\exp(\mathrm{i}(kx+ly+\omega z)), \tag{7}$$

where A is the real amplitude and k and l are the real wave numbers of the carrier wave with ω as real frequency of the wave solution. These parameters are connected through the nonlinear dispersion relation

$$\omega = \frac{2A^2}{q} - \frac{4A^6}{q^3} - \frac{A}{2}[k^2+l^2]. \tag{8}$$

The stability of the aforementioned solution is analyzed by introducing the linear stability ansätz for the perturbed system

$$E = \big[A+\delta u(x,y,z)\big]\exp(\mathrm{i}(kx+ly+\omega z)), \tag{9}$$

where the modulation of the amplitude $\delta u(x,y,z)$ is a small perturbation of the carrier wave and is assumed to be small in comparison with the corresponding parameters of the carrier wave. Inserting Eq. (9) into Eq. (6), after linearization with respect to $\delta u(x,y,z)$, we obtain an equation which describes the evolution of the perturbation

$$\begin{aligned}&\mathrm{i}u_z - \omega u + \frac{1}{2}(u_{xx}+u_{yy}+2\mathrm{i}ku_x+2\mathrm{i}lu_y-k^2u-l^2u)\\&+\frac{2}{q}(2A^2u+A^2u^*)-\frac{4}{q^3}(4A^6u+3A^6u^*)=0.\end{aligned} \tag{10}$$

Further, we choose the modulation ansätz of the following form

$$\begin{aligned}\delta u(x,y,z) \;=\; &\eta_1\exp\big[\mathrm{i}(Kx+Ly-\Omega z)\big]\\&+\eta_2^*\exp\big[-\mathrm{i}(Kx+Ly-\Omega^* z)\big],\end{aligned} \tag{11}$$

in which, K, L represent the wave numbers along x and y directions respectively and Ω is the angular frequency of the perturbation with η_1 and η_2^* being the complex constant amplitudes. Equation (11) represents a combination of progressive and regressive waves. Considering the nonlinear dispersion relation and the preceeding expression of the perturbation, equation (10) leads to the following linear homogeneous system for η_1 and η_2

$$\big[-\Omega+F-2(kK+lL)\big]\eta_1+G\eta_2=0, \tag{12}$$

$$\big[\Omega+F+2(kK+lL)\big]\eta_2+G\eta_1=0, \tag{13}$$

which leads to a second-order equation for Ω

$$\Omega_\pm = -H\pm\sqrt{F^2-G^2}, \tag{14}$$

where

$$\begin{aligned}H &= F-2(kK+lL),\\G &= \frac{2}{q}A^2-\frac{12}{q^3}A^6,\\F &= -\omega-\Big(\frac{K^2+L^2}{2}\Big)-(k^2+l^2)+\frac{4}{q}A^2-\frac{16}{q^3}A^6.\end{aligned}$$

Naturally, equation (10) is modulationally stable for any wave numbers K and L if and only if both Ω_+ and Ω_- are negative. It is evident that for both Ω_+ and Ω_- to be negative, it is necessary that $F^2-G^2\geq 0$ and sufficient that G is positive. Thus, the following inequality is necessary for modulation stability

$$F^2-G^2\geq 0,\;\; F<0, G>0. \tag{15}$$

We then obtain the following criteria for the modulational stability

$$\begin{aligned}\Omega \;=\; &\omega+\Big(\frac{K^2+L^2}{2}\Big)+(k^2+l^2)-\frac{4A^2}{q}+\frac{16A^2}{q^3}+2(kK+lL)\\&\pm\sqrt{\Big[-\omega-\Big(\frac{K^2+L^2}{2}\Big)-(k^2+l^2)+\frac{4A^2}{q}-\frac{16A^6}{q^3}\Big]^2-\Big(\frac{2A^2}{q}-\frac{12A^6}{q^3}\Big)^2}.\end{aligned} \tag{16}$$

We note that if some wave numbers K of the conditions expressed in Eq. (15) are violated, i.e., $F^2-G^2>0$, then consequently

Eq. (6) is modulationally unstable and the perturbation growth rate reads as

$$g(\Omega) \equiv \mathrm{Im}(\Omega) \equiv \pm\sqrt{\left(\frac{2A^2}{q} - \frac{12A^6}{q^3}\right)^2 - \left[-\omega - \left(\frac{K^2+L^2}{2}\right) - (k^2+l^2) + \frac{4A^2}{q} - \frac{16A^6}{q^3}\right]^2}. \tag{17}$$

The gain exhibits a more interesting dependence of Ω on the parameter q which is related to the strength of the external static electric field. Linear stability analysis can determine the instability domain in parameter space and predicts qualitatively how the amplitude of a modulation side band evolves at the onset of the instability. Figure 2 portrays the stability/instability domains in the (k,K) plane and the corresponding influence of the parameter q for the parametric choices $\omega = 1, l = 1, L = 1$, and $A = 1$. In these figures, the dark bluish area corresponds to a region where the nonlinear plane waves are stable with respect to the modulation of any wave number K and the region with bright yellowish orange area experiences in which the amplitude of any wave would be expected to suddenly display an exponential growth. From Fig. 2, it is obvious that the domain of instability seems to be reduced appreciably as an impact of the applied external field. Figure 3 depicts the plot of the modulational instability gain in the (k,K) plane for various values of q, verifying the above described fact. We also plot the growth rate in the (A,K) plane as shown in Fig. 4 for various values of the applied electric field and we observe that, upon increasing the value of q, the nonlinear propagating plane waves are highly localized via modulational instability and the corresponding MI gain spectrum is also depicted in Fig. 5. It is inferred from Fig. 5 that a low value of optimized electric field is sufficient enough to trigger instability in an NLC system which leads to the localization of propagating nonlinear plane wave in the medium.

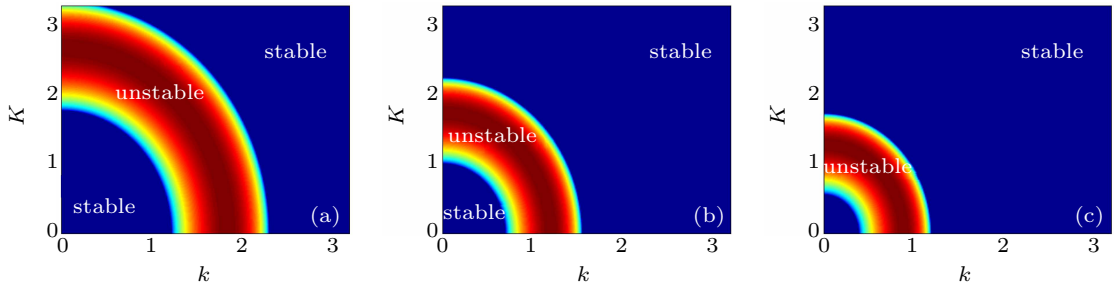


Fig. 2. (color online) Gain spectrum of the MI gain in (k,K) plane for the parametric choices $\omega = 1$, $l = 1$, $L = 1$, and $A = 1$. Panel (a) for $q = 0.1$, (b) for $q = 0.5$, and (c) $q = 1.0$.

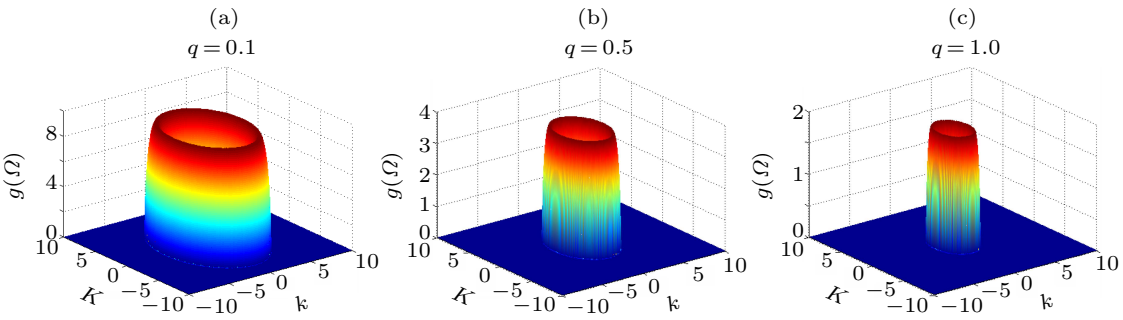


Fig. 3. (color online) The modulational instability (MI) gain (Eq. 17) in (k,K) plane for the parametric values of $\omega = 1$, $l = 1$, $L = 1$, and $A = 1$.

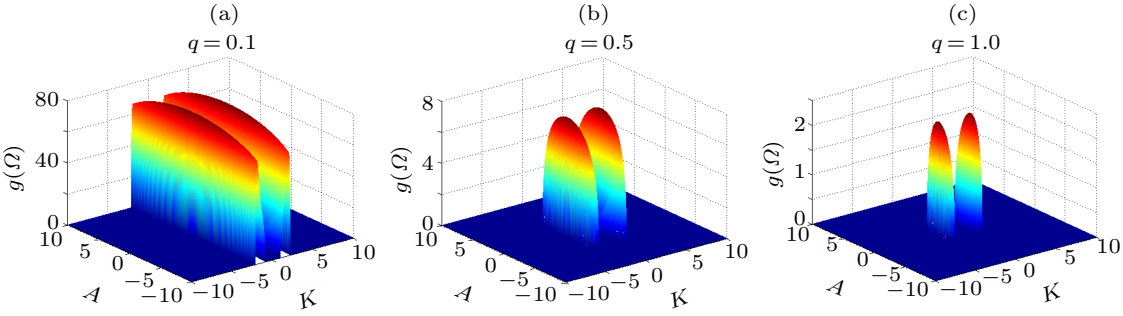


Fig. 4. (color online) Snapshots of the instability domains of MI gain spectra for (A,K) plane.

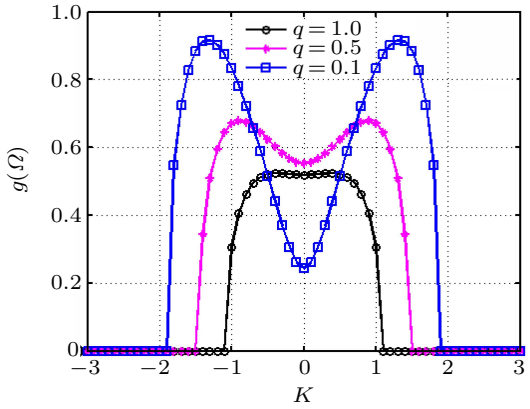


Fig. 5. (color online) Modulational instability gain spectra in 2D representation for various values of q.

4. Exact soliton solution of the higher order NLS equation

In this section, we invoke the homogeneous balance (HB) method and the exponential function method to solve the higher order NLS equation (6).

4.1. Periodic soliton solutions through homogeneous balance method

Nonlinear evolution equations are often used as models to describe the complex phenomena in various fields of sciences, especially in physics and engineering. One of the basic physical problems for those models is to find their traveling wave solutions. During the past decades, quite a few methods for dealing with traveling wave solutions of those nonlinear equations have been proposed.[33–57] In the past several decades, both mathematicians and physicists have made a significant progress in this direction. Recently, Wang *et al.*[58,59] presented a powerful homogeneous balance (HB) method for finding exact solitary wave solutions of a given nonlinear partial differential equation. Fan[60] used the HB method to search for Bäcklund transformation and similarity reduction of nonlinear partial differential equations. In addition, he showed that there is a close connection among the HB method, Weiss, Tabor, Carnevale (WTC) method, and Clarkson, Kruskal (CK) methods. El-Wakil *et al.*[33] used the homogeneous balance method to construct the auto-Bäcklund transformation for the generalized shallow water wave equation and generalized variable coefficient 2D Korteweg-de Vries (KdV) equation and found new exact solitary wave solutions. However, they investigated the travelling wave solutions for a class of nonlinear evolution equations, in which the homogeneous balance method was applied to solve the Riccati equation and the reduced nonlinear evolution equations. Here, we use the homogeneous balance method to solve the Riccati equation $\phi' = b\phi + d$ and the reduced nonlinear ordinary differential equation, respectively. It makes the homogeneous balance method be used more extensively and the method is called the extended homogeneous balance method since the homogeneous balance method is used twice.

To look for traveling wave solutions of Eq. (6), we make the following transformation

$$E = u(\xi)\exp(\mathrm{i}\theta), \quad \theta = \alpha x - \beta z + \gamma y,$$
$$\xi = \alpha_1 x + \beta_1 z + \gamma_1 y, \tag{18}$$

where α, β, γ, α_1, β_1, and γ_1 are arbitrary constants and substituting Eq. (18) into Eq. (6) thereby separating the real part from the complex form of nonlinear ordinary differential equations, we obtain

$$-\beta u + \frac{1}{2}\left[u_{\xi\xi}(\alpha_1^2+\gamma_1^2) - u(\alpha^2+\gamma^2)\right] + \frac{2}{q}u^3 - \frac{4}{q^3}u^7 = 0, \tag{19}$$

$$cu_\xi + u_\xi(\alpha_1\alpha + \gamma_1\gamma) = 0. \tag{20}$$

The next crucial step is to look for the solution of Eq. (6) in the form

$$u(\xi) = \sum_{i=0}^{n} a_i \phi^i, \tag{21}$$

where a_i are the constants to be determined and ϕ satisfies the following Riccati equation

$$\phi' = b\phi + d, \tag{22}$$

where b and d are constants. Balancing the highest order derivative term with the nonlinear term in Eq. (19) gives leading order $n = 1$. Therefore, we rewrite Eq. (21) as

$$u(\xi) = a_0 + a_1\phi. \tag{23}$$

Substituting Eq. (23) into Eqs. (19) and (20) along with Eq. (22) and collecting all the terms with the same power in $\phi^i\,(i = 1, 2, \ldots)$ yields a set of algebraic system of equations given by

$$\begin{aligned}
&-4a_1^7 = 0, \quad -28a_0a_1^6 = 0, \quad -84a_0^2a_1^5 = 0, \quad -140a_0^3a_1^4 = 0,\\
&2qa_1^3 + \gamma_1^2a_1q^3 + \alpha_1^2a_1q^3 - 140a_0^4a_1^3 = 0,\\
&-84a_0^5a_1^2 + 6qa_0a_1^2 = 0,\\
&6qa_0^2a_1 - \frac{1}{2}\alpha^2q^3a_1 + \alpha_1^2a_1q^3b - 28a_0^6a_1\\
&\qquad - \frac{1}{2}\gamma^2q^3a_1 + \gamma_1^2a_1q^3b - \beta q^3a_1 = 0,\\
&-\beta q^3a_0 - 4a_0^7 + 2qa_0^3 - \frac{1}{2}\alpha^2q^3a_0 - \frac{1}{2}\gamma^2q^3a_0 = 0.
\end{aligned} \tag{24}$$

Solving these algebraic equations with the aid of MATLAB, we find the solution as follows:

$$a_0 = \left[\frac{q}{14}\right]^{1/4}, \quad a_1 = \frac{\sqrt{qb^2(\gamma_1^2+\alpha_1^2)}}{2\sqrt{2}}, \quad b = b, d = d. \tag{25}$$

It is to be noted that the Riccati equation (22) can be solved using the homogeneous balance method as follows.

Case 1 Let us assume that $\phi = \sum_{i=0}^{m}\tau_i\tanh^i(\xi)$. Balancing the highest derivative term with the nonlinear term leads to

$$\phi = -\frac{1}{a}\tanh(\xi), \quad ac = -1. \tag{26}$$

Substituting Eqs. (25) and (26) into Eqs. (23) and (18) gives

rise to the exact traveling wave solutions of Eq. (6) as follows:

$$E = \left[\left[\frac{q}{14}\right]^{1/4} - \frac{\sqrt{qb^2(\gamma_1^2+\alpha_1^2)}}{2\sqrt{2}}\tanh(\xi)\right]\exp(\mathrm{i}\theta). \quad (27)$$

The above solution assumes the form of bell-shaped solitary excitations. Similarly, choosing

$$\phi = \sum_{i=0}^{m} \tau_i \coth^i(\xi),$$

we obtain the following new traveling wave soliton solution of Eq. (6)

$$E = \left[\left[\frac{q}{14}\right]^{1/4} - \frac{\sqrt{qb^2(\gamma_1^2+\alpha_1^2)}}{2\sqrt{2}}\coth(\xi)\right]\exp(\mathrm{i}\theta). \quad (28)$$

In Fig. 6, we plot Eq. (28) for the set of parameters $y = 0.1$, $\alpha = 1$, $\beta = 1$, $\gamma = 2$, $\alpha_1 = 0.01$, $c = 0.5$, $\beta_1 = 1$, $\gamma_1 = 0.1$, and $b = 0.1$. In order to explore the role of the external electric field on the localized solutions, we vary the value of q from 0.0005 to 4 and observe that the antisolitonic profile is gradually changing its shape to antikink form as shown in Fig. 6.

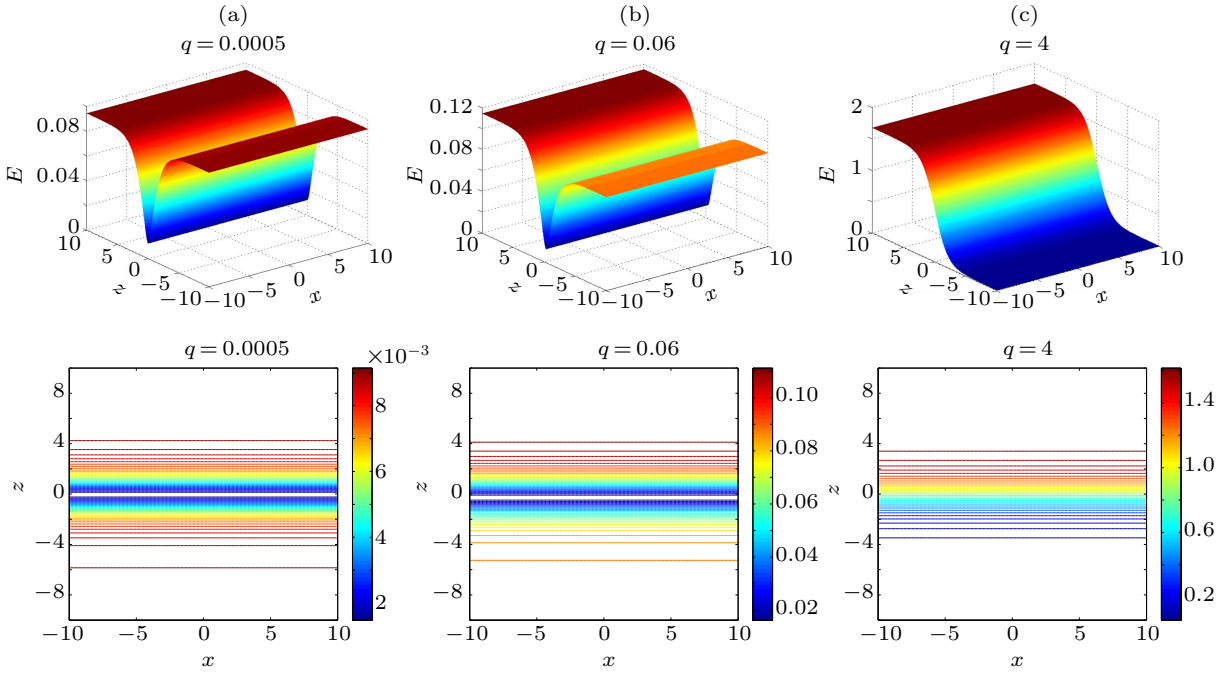


Fig. 6. (color online) Snapshots of shape-changing soliton profiles for various values of the applied electric field (q) with the parametric values $y = 0.1$, $\alpha = 1$, $\beta = 1$, $\gamma = 2$, $\alpha_1 = 0.01$, $c = 0.5$, $\beta_1 = 1$, $\gamma_1 = 0.1$, and $b = 0.1$.

Case 2 Next, we consider the case $d < 0$ and $b = 1$, then the Riccati equation (22) yields the following solution

$$\phi = -\sqrt{-d}\tanh(\sqrt{-d}\xi). \quad (29)$$

From Eqs. (25), (29), and (18), we have the following new traveling wave solutions of higher order NLS equation (6), which contain traveling wave solutions, periodic wave solutions, and rational solutions as follows:

$$E = \left[\left[\frac{q}{14}\right]^{1/4} + \frac{\sqrt{qb^2(\gamma_1^2+\alpha_1^2)}}{2\sqrt{2}}\sqrt{-d}\tanh(\sqrt{-d}\xi)\right]\exp(\mathrm{i}\theta). \quad (30)$$

If $d < 0$, we have

$$E = \left[\left[\frac{q}{14}\right]^{1/4} - \frac{\sqrt{qb^2(\gamma_1^2+\alpha_1^2)}}{2\sqrt{2}}\sqrt{d}\tanh(\sqrt{d}\xi)\right]\exp(\mathrm{i}\theta). \quad (31)$$

Figure 7 portrays the snapshots of the periodic solitons of Eq. (30) with multiple humps for the parametric choices $y = 2$, $\alpha = 2$, $\beta = 0.1$, $\gamma = 2$, $\alpha_1 = 0.6$, $c = 0.2$, $\beta_1 = 1$, $\gamma_1 = 1$, and $b = 0.01$. From the figure, we could observe that under the influence of the external electric field q which takes values as $q = 0.1$ and $q = 0.7$, the soliton with periodic multiple humps stays as such but with an increased amplitude as shown in Fig. 7.

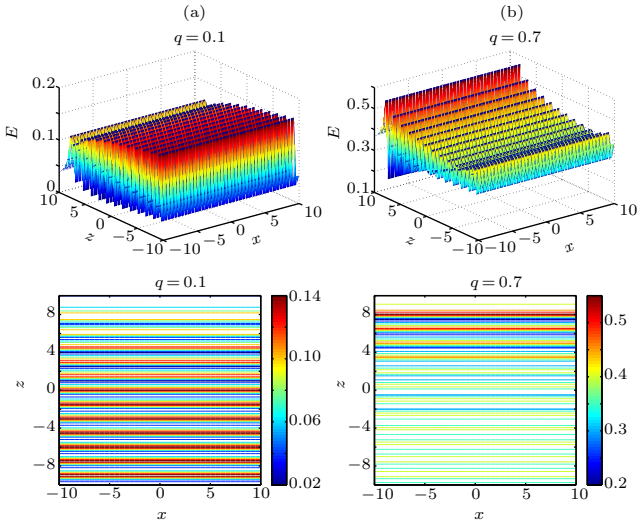


Fig. 7. (color online) Periodic behavior of solitonic profile for various values of q for the choices of parametric values $y = 2, \alpha = 2, \beta = 0.1, \gamma = 2, \alpha_1 = 0.6, c = 0.2, \beta_1 = 1, \gamma_1 = 1$, and $b = 0.01$.

Case 3 We suppose that the Riccati equation (22) has the following solutions of the form

$$\phi = \sum_{i=0}^{m} (A_i f^i + B_i f^{i-1} g), \tag{32}$$

with

$$f = \frac{1}{\cosh\xi + r}, \quad g = \frac{\sinh\xi}{\cosh\xi + r}, \tag{33}$$

and balancing the highest derivative term with a nonlinear term leads to

$$\phi = A_0 + A_1 f + B_1 g. \tag{34}$$

Substituting Eq. (34) into Eq. (22), and collecting the coefficients of the same power $f^i g^i$ and setting each of the obtained coefficients to zero we obtain the set of algebraic equations. The resultant algebraic equations leads to

$$\phi = \frac{1}{2b} \pm \frac{\sqrt{r^2-1} - \sinh\xi}{\cosh\xi + r}. \tag{35}$$

Substituting Eqs. (35) and (25) into Eq. (18), we obtain the new wave solutions of Eq. (6) as

$$E = \left[\left[\frac{q}{14}\right]^{1/4} - \frac{\sqrt{qb^2(\gamma_1^2+\alpha_1^2)}}{4\sqrt{2}b} \frac{\sqrt{r^2-1} - \sinh\xi}{\cosh\xi + r}\right] \exp(\mathrm{i}\theta). \tag{36}$$

We plot Eq. (36) for various values of q and also for the parametric choices $y = \pi/2$, $\alpha = 2$, $\beta = 1$, $\gamma = 2$, $\alpha_1 = 0.2$, $c = 3$, $\gamma_1 = 1$, $b = 1$, $r = 1$, and $\beta_1 = 1$ and surprisingly, we observe from Fig. 8(a), that initially for the value of $q = 1.56$, the localized profile assumes the form of a soliton with oscillatory humps with the tails resting at the minimum amplitude. However, when $q = 1.5$, the same solitonic profile with the same oscillatory humps exhibits small fluctuations at both the tails which is not resting at the minimum amplitude in this case as shown in Fig. 8(b), gradually leading to a hybrid form of soliton-kink profile. Further, when $q = 1.43$, the solitonic-kink on hybrid profile, slowly assumes the form of an anti-kink profile with oscillatory humps as depicted in Fig. 8(c).

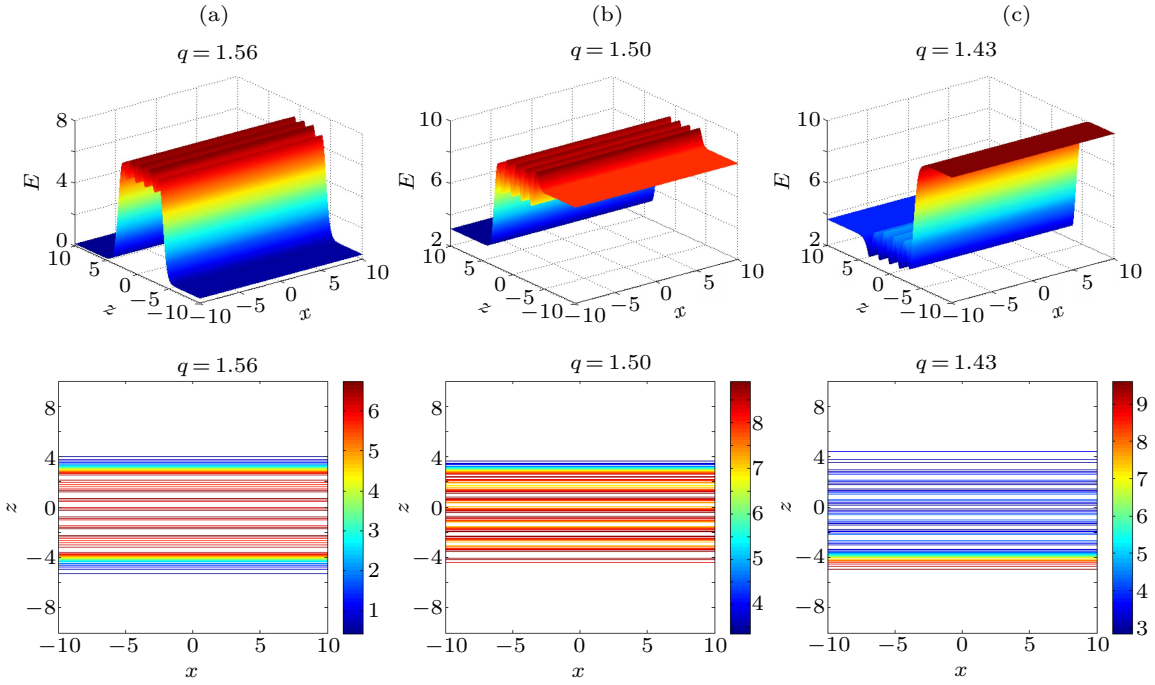


Fig. 8. (color online) Snapshots of the hybrid solitonic profile for the choices of parameters $y = \pi/2$, $\alpha = 2$, $\beta = 1$, $\gamma = 2$, $\alpha_1 = 0.2$, $c = 3$, $\gamma_1 = 1$, $b = 1$, $r = 1$, and $\beta_1 = 1$ for various values of q.

Case 4 In this case, let us take ϕ in the Riccati equation (22) as

$$\phi = \exp(p_1\xi)\rho(z) + p_4(\xi), \quad \text{where} \quad z = \exp(p_2\xi)p_3, \tag{37}$$

and p_1, p_2, and p_3 are constants to be determined. Substituting Eq. (37) into Eq. (22), we find that when $c = -p_1^2/(4a)$

$$\phi = -\frac{p_1 \mathrm{e}^{p_1\xi}}{a(\mathrm{e}^{p_1\xi} + p_3)}. \tag{38}$$

If $p_3 = 1$ in Eq. (38), we obtain

$$\phi = -\frac{p_1}{2a}\tanh\left(\frac{p_1\xi}{2}\right). \tag{39}$$

If $p_3 = -1$ in Eq. (39), we obtain

$$\phi = -\frac{p_1}{2a}\coth\left(\frac{p_1\xi}{2}\right). \tag{40}$$

When $p_3 = 1$, using Eq. (18), it yields

$$E = \left[\left[\frac{q}{14}\right]^{1/4} + \frac{\sqrt{sb^2(\gamma_1^2+\alpha_1^2)}}{4\sqrt{2}b}\tanh\left(\frac{p_1\xi}{2}\right)\right]\exp(\mathrm{i}\theta). \tag{41}$$

When $p_3 = -1$, and also from Eq. (18)

$$E = \left[\left[\frac{qs}{14}\right]^{1/4} + \frac{\sqrt{sb^2(\gamma_1^2+\alpha_1^2)}}{4\sqrt{2}b}\coth\left(\frac{p_1\xi}{2}\right)\right]\exp(\mathrm{i}\theta). \tag{42}$$

In Fig. 9, we have plotted Eq. (41), for the choices of parameters $y = \pi/2$, $\alpha = 2$, $\beta = 1$, $\gamma = 2$, $\alpha_1 = 0.2$, $c = 9$, $\gamma_1 = 1$, $b = 1$, $\beta_1 = 1$, $a = 1$, and $p_1 = 0.1$. Upon increasing the strength of the applied electric field, the solution takes the form of dark soliton further transforming into a bright soliton when $q = 0.3$. These shape changing localized solitary profiles admit the propagation of laser light in an NLC medium.

From the physical point of view, these optically induced spatial solitons in nematic liquid crystals possess immense applications in all-optical switching and optical reconfigurable interconnects by means of soliton interactions.[61] Owing to their ability to self-trap as well as to guide weaker signals within the wave guide or light-pipes, these optically induced spatial solitons could form the basis of future all-optical processing networks. One of the most interesting features in the communication field is the lossless energy transfer in the form of nematicons which can be used for fiber-to-fiber interaction processes.[62,63]

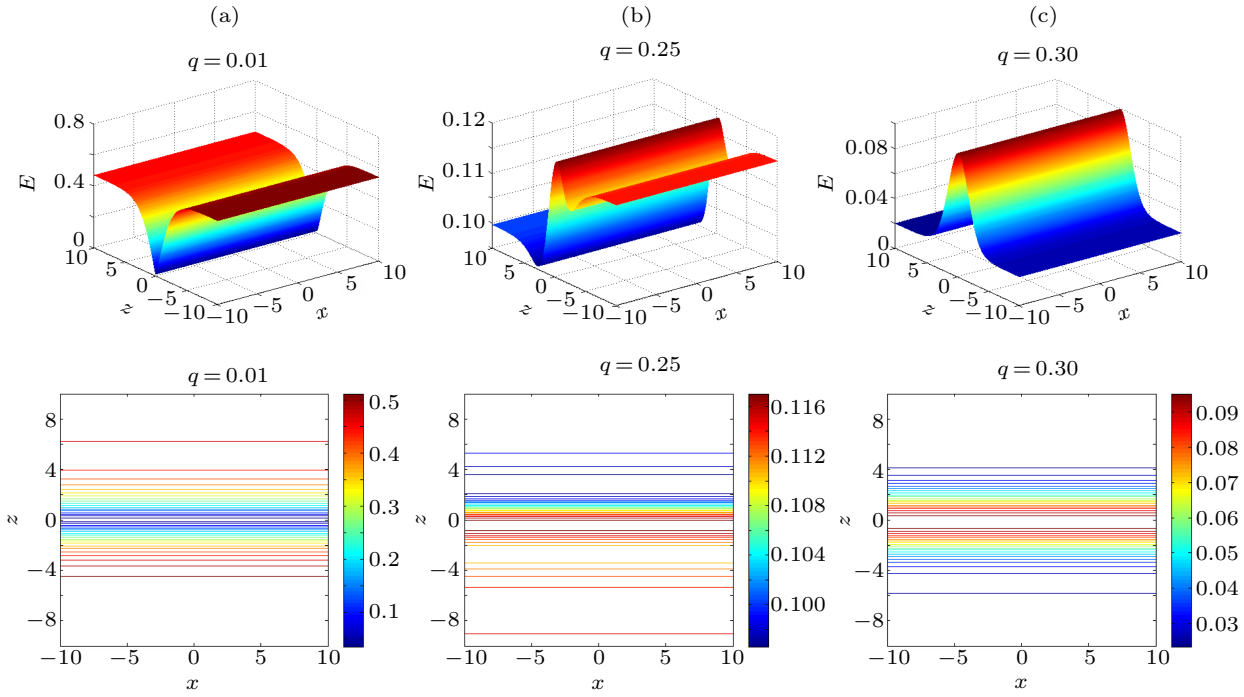


Fig. 9. (color online) Snapshots of dark to bright soliton profiles of Eq. (41) with the parameters $y = \pi/2$, $\alpha = 2$, $\beta = 1$, $\gamma = 2$, $\alpha_1 = 0.2$, $c = 9$, $\gamma_1 = 1$, $b = 1$, $\beta_1 = 1$, $a = 1$, and $p_1 = 0.1$.

4.2. Exact soliton solution through Exp-function method

Among the wealth of methods available for solving NLPDEs, one of the most straightforward, concise, and effective algorithms aided with symbolic computation is the Exp-function method. It is a novel approach first proposed by He and Wu[64] to solve the nonlinear evolution equations with high nonlinearity. Further, through numerous investigations in the past decades, He[65] has studied the concepts of the recently developed asymptotic methods including the exponential function method. The basic idea of the Exp-function method was presented in He's monograph[66] and is used by many researchers to study various NLPDEs including higher dimensional equations. This work has initiated an enormous research[67,68] in the scientific community. The important remarks of the Exp-function method have been described in Refs. [64] and [67] which illustrates that the method yields the generalized solutions of both solitary and periodic nature. Moreover, the expression of the Exp-function is more general than the sine and tangent hyperbolic functions, so that one can find the explicit form of the more general solutions in the Exp-function method. Also, the symbolic computational packages like Maple, Mathematica, and Matlab make the solution procedure of Exp-function so simple, concise, and time conceptual. The implementation of the method to the nonlinear wave equation can be done both straightforwardly and by the sub-equation way. But the direct use of the method is preferable because of not only its convenience, but also the possibility of losing some information which occurs while using the method of sub-equation. Therefore, the Exp-function method is more convenient and effective than the extended Fan sub-equation method and thus becomes a promising and powerful method in dealing with the nonlinear evolution equations. Very recently, Marinakis[69] and Zhang *et al.*[38] have constructed the N-soliton solutions for the nonlinear evolution equation using Exp-function method. It is worth enough to point out that the method is also valid for difference–differential equations.[71,72] It is revealed from these studies that the free parameters in the solutions obtained using Exp-function can recover some known solutions found by the most existing methods. To illustrate the essential idea of this method

in Refs. [73] and [74], we construct the more generalized wave solution of the higher order NLS equation (6) by invoking Exp-function method.

Next, we assume the traveling wave ansätz containing Exp-function for u expressed in the form[64]

$$u(\xi)=\frac{\sum_{n=-c}^{d}a_n\exp(n\xi)}{\sum_{m=-p}^{q}b_m\exp(m\xi)}, \tag{43}$$

where m, n, p, and q are unknown positive integers which could be freely chosen and a_n, b_m are unknown constants to be determined. In order to determine the values of c and p, we balance the linear term of higher order $u_{\xi\xi}$ with the highest order nonlinear term u^3 in Eq. (19) and upon some algebraic manipulations, we have

$$u_{\xi\xi}=\frac{A_1\exp[-(3p+c)\xi]+\cdots}{A_2\exp[-4p\xi]+\cdots},$$

and

$$u^3=\frac{B_1\exp[-(3c+p)\xi]+\cdots}{B_2\exp[-4p\xi]+\cdots},$$

where A_i and B_i are the determined coefficients. Now, equating the highest order of the exponential function term in the above expression, we have $-(3p+c)=-(3c+p)$, which leads to the result $p=c$. In a similar manner, balancing the lowest order in Eq. (19), we have

$$u_{\xi\xi}=\frac{\cdots+C_1\exp[(3q+d)\xi]}{\cdots+C_2\exp[4q\xi]},$$

and

$$u^3=\frac{\cdots+D_1\exp[(3d+q)\xi]}{\cdots+D_2\exp[4q\xi]}.$$

Here, C_i and D_i are also the determined coefficients. Again, equating the powers of exponential terms, we obtain the following relation $(3q+d)=(3d+q)$ resulting in $q=d$. The values of c, d, p, and q can be freely chosen in general and for convenience, we consider

$$p=c=q=d=1.$$

Therefore, the traveling wave solution for u can be written as

$$u=\frac{a_{-1}\exp(-\xi)+a_0+a_1\exp(\xi)}{b_{-1}\exp(-\xi)+b_0+b_1\exp(\xi)}. \tag{44}$$

Inserting Eq. (44) into Eq. (19) which yields the following set of algebraic equations in powers of exponential terms:

$$\begin{aligned}&P_1\exp(\xi)+P_2\exp(2\xi)+P_3\exp(3\xi)+P_4\exp(4\xi)\\&+P_5\exp(5\xi)+P_6\exp(6\xi)+P_7\exp(7\xi)+P_{-1}\exp(-\xi)\\&+P_{-2}\exp(-2\xi)+P_{-3}\exp(-3\xi)+P_{-4}\exp(-4\xi)\\&+P_{-5}\exp(-5\xi)+P_{-6}\exp(-6\xi)+P_{-7}\exp(-7\xi)=0,\end{aligned} \tag{45}$$

where P_i $(i=\pm1,\ldots,\pm7)$ are the determined coefficients which are not written down explicitly here. Equating the coefficients of exponential terms to zero, we obtain the series of equations as follows:

$$\begin{aligned}&P_{\pm1}=0,\\&P_{\pm2}=0,\\&\cdots\\&P_{\pm7}=0.\end{aligned}$$

Using the above choices of parameters in Eq. (44) and by solving the above set of equations using a systematic algebraic symbolic computation, we obtain an exact localized solution as given below

$$a_1=\frac{b_1a_0}{b_0},\quad b_1=b_1,\quad a_{-1}=\frac{\left[\begin{array}{c}-3a_0(-4q^2a_0^2a_1b_1^4+56a_0^2a_1^5+5\gamma^2q^3a_1b_0^2b_1^4+\alpha_1^2q^3a_1b_0^2b_1^4\\+5\alpha^2q^3a_1b_0^2b_1^4+10\beta q^3a_1b_0^2b_1^4+\gamma_1^2q^3a_1b_0^2b_1^4\\-16q^2a_0a_1^2b_0b_1^3-\alpha_1^2q^3a_0b_0b_1^5+2\alpha^2q^3a_0b_0b_1^5\\+4\beta q^3a_0b_0b_1^5-\gamma_1^2q^3a_0b_0b_1^5+2\gamma^2q^3a_0b_0b_1^5\\-8q^2a_1^3b_0^2b_1^2)\end{array}\right]}{\left[\begin{array}{c}(56a_1^6a_0+12q^3a_1b_1^5b_0\beta+4q^3a_1b_1^5b_0\alpha_1^2+6q^3a_1b_1^5b_0\alpha^2\\+4q^3a_1b_1^5b_0\gamma_1^2+6q^3a_1b_1^5b_0\gamma^2+2\beta q^3b_1^6a_0\\+\alpha^2q^3b_1^6a_0-4\gamma_1^2q^3b_1^6a_0-4\alpha_1^2q^3b_1^6a_0\\+\gamma^2q^3b_1^6a_0-12q^2a_1^2b_1^4a_0-16q^2a_1^3b_1^3b_0)\end{array}\right]},$$

$$b_{-1}=\frac{\left[\begin{array}{c}-(3(-4q^2a_0^2a_1b_1^4+56a_0^2a_1^5+5\gamma^2q^3a_1b_0^2b_1^4+\alpha_1^2q^3a_1b_0^2b_1^4\\+5\alpha^2q^3a_1b_0^2b_1^4+10\beta q^3a_1b_0^2b_1^4+\gamma_1^2q^3a_1b_0^2b_1^4\\-16q^2a_0a_1^2b_0b_1^3-\alpha_1^2q^3a_0b_0b_1^5+2\alpha^2q^3a_0b_0b_1^5\\+4\beta q^3a_0b_0b_1^5-\gamma_1^2q^3a_0b_0b_1^5+2\gamma^2q^3a_0b_0b_1^5\\-8q^2a_1^3b_0^2b_1^2))b_0\end{array}\right]}{\left[\begin{array}{c}(56a_1^6a_0+12q^3a_1b_1^5b_0\beta+4q^3a_1b_1^5b_0\alpha_1^2+6q^3a_1b_1^5b_0\alpha^2\\+4q^3a_1b_1^5b_0\gamma_1^2+6q^3a_1b_1^5b_0\gamma^2+2\beta q^3b_1^6a_0\\+\alpha^2q^3b_1^6a_0-4\gamma_1^2q^3b_1^6a_0-4\alpha_1^2q^3b_1^6a_0\\+\gamma^2q^3b_1^6a_0-12q^2a_1^2b_1^4a_0-16q^2a_1^3b_1^3b_0)\end{array}\right]}.$$

Using the above choices of parameters in Eqs. (45) and (18), one can obtain

$$E=\frac{(-3a_0p/q)\exp[-(\alpha_1x+\beta_1z+\gamma_1y)]+a_0+(b_1a_0/b_0)\exp(\alpha_1x+\beta_1z+\gamma_1y)}{(-3b_0p/q)\exp[-(\alpha_1x+\beta_1z+\gamma_1y)]+b_0+b_1\exp(\alpha_1x+\beta_1z+\gamma_1y)}\exp[\mathrm{i}(\alpha x-\beta z+\gamma y)], \tag{46}$$

where

$$
\begin{aligned}
p = & -4q^2a_0^2a_1b_1^4 + 56a_0^2a_1^5 + 5\gamma^2q^3a_1b_0^2b_1^4 + \alpha_1^2q^3a_1b_0^2b_1^4 \\
& + 5\alpha^2q^3a_1b_0^2b_1^4 + 10\beta q^3a_1b_0^2b_1^4 + \gamma_1^2q^3a_1b_0^2b_1^4 \\
& - 16q^2a_0a_1^2b_0b_1^3 - \alpha_1^2q^3a_0b_0b_1^5 + 2\alpha^2q^3a_0b_0b_1^5 \\
& + 4\beta q^3a_0b_0b_1^5 - \gamma_1^2q^3a_0b_0b_1^5 + 2\gamma^2q^3a_0b_0b_1^5 \\
& - 8q^2a_1^3b_0^2b_1^2, \\
q = & \, 56a_1^6a_0 + 12q^3a_1b_1^5b_0\beta + 4q^3a_1b_1^5b_0\alpha_1^2 + 6q^3a_1b_1^5b_0\alpha^2 \\
& + 4q^3a_1b_1^5b_0\gamma_1^2 + 6q^3a_1b_1^5b_0\gamma^2 + 2\beta q^3b_1^6a_0 + \alpha^2q^3b_1^6a_0 \\
& - 4\gamma_1^2q^3b_1^6a_0 - 4\alpha_1^2q^3b_1^6a_0 + \gamma^2q^3b_1^6a_0 - 12q^2a_1^2b_1^4a_0 \\
& - 16q^2a_1^3b_1^3b_0.
\end{aligned}
$$

Thus, we find that the higher order nonlinear Schrödinger equation (6) admits, the coherent dark-soliton solutions using the exponential function method. In order to understand the physical nature of the nematicon formation which originates from the interaction between high intensity optical beam and molecular orientation in NLC system, we have displayed the pictorial representation of the solution (Eq. (46)) for the choices of parameters $y = 0.1$, $\alpha = 1$, $\beta = 1$, $\gamma = 2$, $\alpha_1 = 0.01$, $c = 0.5$, $\beta_1 = 1$, and $\gamma_1 = 0.1$ in Fig. 10. When the relative strength of static to dynamic electric field $q = 0.0005$, the solution of Eq. (6) admits the dark-solitonic profile as displayed in Fig. 10(a), and when $q = 0.06$, the solution assumes the hybrid form of antisoliton-kink profile as shown in Fig. 10(b). Upon tuning the value of $q = 4$ further, it leads to the formation of kink-soliton in Fig. 10(c) and the corresponding contour plots are portrayed in the bottom panel of Fig. 10. We also have compared the solutions Eqs. (28) and (46) obtained by both of the methods and presented them in Fig. 11. Surprisingly one could observe that when the relative strength of the static to dynamic electric field $q = 0.0005$, both the methods exhibit antisolitonic excitations as portrayed in Fig. 11(a). Also when the value of q is tuned to $q = 0.06$, the HB method exhibits the hybrid antisoliton-antikink profile and the Exp-function method exhibits the hybrid phase of antisoliton-kink profile excitations. Ironically, when $q = 4$, the HB method portrays the antikink whereas the Exp-function method portrays the kink profile of excitations.

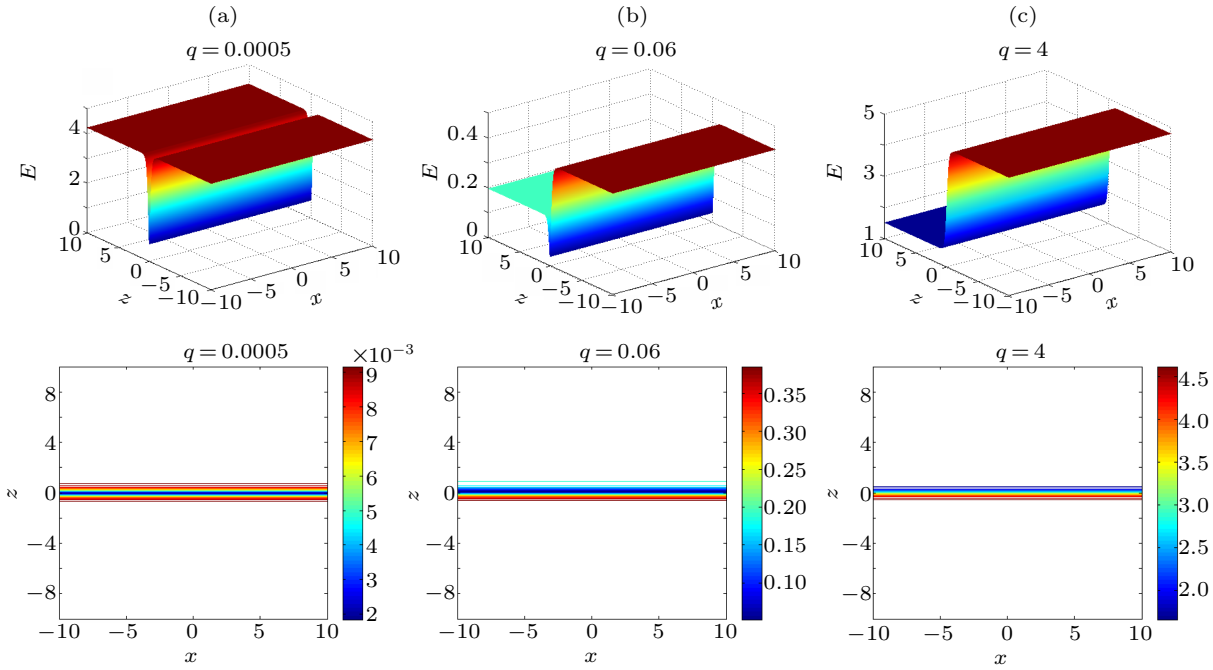


Fig. 10. (color online) Snapshots of dark soliton to kink soliton profiles of Eq. (46) with the parameters $y = 0.1$, $\alpha = 1$, $\beta = 1$, $\gamma = 2$, $\alpha_1 = 0.01$, $c = 0.5$, $\beta_1 = 1$, and $\gamma_1 = 0.1$.

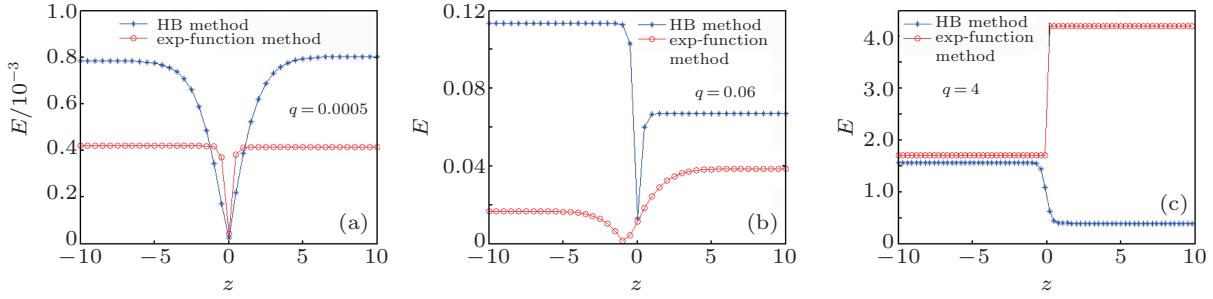


Fig. 11. (color online) The comparison of the solutions E of the two methods (homogeneous balance and Exp-function method) at $x = \pi/2$.

5. Conclusions

The propagation of solitons of coherent polarized light, so-called nematicons, in nematic liquid crystal medium with a local response to reorientation by light is studied. A set of explicit criteria of modulational instability is derived and analyzed. We demonstrate that the stage of the exponential growth of instabilities revealed by the linear stability analysis is highly influenced by the strength of the applied electric field. We also constructed a series of periodic nematicon profiles through the homogeneous balance method and Exp-function method admitting the propagation of laser light in an NLC medium. These optically induced nematicons have been proposed as building blocks in future ultra-fast all-optical devices.

Acknowledgments

One of the authors (L. Kavitha) gratefully acknowledges the financial support from NBHM, India in the form of major research project, BRNS, India in the form of Young Scientist Research Award and ICTP, Italy in the form of Junior Associateship. He also extends his sincere thanks to UGC, India for financial assistance in the form of Research Award. M. Venkatesh acknowledges BSR-Research Fellowship under UGC Non-SAP Scheme, India. S. Dhamayanthi thanks the University Research Fellowship (URF) given by Periyar University, India.

References

[1] Dodd R K, Eilbeck J C, Dibbon J D and Morris H C 1982 *Solitons and Nonlinear Wave Equation* (New York: Academic Press)
[2] Drazin P G and Johnson R S 1989 *Solitons: An Introduction* (New York: Cambridge University Press)
[3] Stegeman G I, Christodoulides D N and Sege M 2000 *IEEE J. Sel. Top. Quantum Electron* **6** 1419
[4] Kivshar Y S and Agrawal G P 2003 *Optical Solitons: From Fibers to Photonic Crystals* (New York: Academic)
[5] Peccianti M, Dyadyusha A, Kaczmarek M and Assanto G 2006 *Nat. Phys.* **2** 737
[6] Shalaby M and Barthelemy A 1991 *Opt. Lett.* **16** 1472
[7] Shen Y R 2002 *The Principle of Nonlinear Optics* (New York: Wiley)
[8] Khoo I C 1995 *Liquid Crystals: Physical Properties and Nonlinear Optical Phenomena* (New York: Wiley)
[9] Daniel M, Gnanasekaran K and Kavitha L 2008 *Physica D* **237** 3135
[10] Assanto G and Peccianti M 2003 *IEEE J. Quantum Electron* **39** 13
[11] Mclaughlin D W, Muraki D J, Shelley M J and Wang X 1995 *Physica D* **88** 55
[12] McLaughlin D W, David J M and Michael J S 1996 *Physica D* **97** 471
[13] Conti C, Peccianti M and Assanto G 2003 *Phys. Rev. Lett.* **91** 073901
[14] Catherine G R, Antonmaria A M, Marchant T R, Noel F S and Annette L W 2008 *Physica D* **237** 1088
[15] Collet J H, Litaize D, van Camenhout J, Jesshope C, Desmulliez M, Thienpont H, Goodman J W and Louri A 2000 *Appl. Opt.* **39** 671
[16] Pinkston T M and Goodman J W 1994 *Appl. Opt.* **33** 1434
[17] Yang L, Liu J and Wang K 2001 *Phys. Lett. A* **278** 267
[18] de Gennes P G and Prost J 1974 *The Physics of Liquid Crystals* (Oxford: Clarendon Press)
[19] Snyder A and Mitchell D 1997 *Science* **276** 1538
[20] Reyes J A and Palffy-Muhoray P 1998 *Phys. Rev. E* **58** 5855
[21] Sarkissian H, Tsai C, Zeldovich B and Tabirian N 2005 *"Beam Clean Up and Combining Using Orientational Stimulated Scattering in Liquid Crystal"*, Conference on Laser and Electro–Optics: Application of LY3 Nonlinearities, Optical Society of America, 2005, p. 505
[22] Warenghem M, Blach J F, Henninot J F 2006 *Mol. Cryst. Liq. Cryst.* **454** 297
[23] Reinbert C G, Minzoni A A, Smyth N F and Worthy A L 2006 *J. Opt. Soc. Am. B* **23** 2551
[24] Reinbert C G, Minzoni A A and Smyth N F 2006 *J. Opt. Soc. Am. B* **23** 294
[25] Fratalocchi A and Assanto G 2005 *Phys. Rev. E* **72** 066608
[26] Krolikowski W, Bang O, Nikolov N, Neshev D, Wyller J, Ramussen J and Edmundson D 2004 *J. Opt. B* **6** S288
[27] Wyller J, Krlikowski W Z, Bang O, Petersen D E and Rasmussen J J 2007 *Physica D* **227** 8
[28] Griffiths S D, Grimshaw R H J and Khusnutdinova K R 2006 *Physica D* **214** 1
[29] Li S C and Duan W S 2009 *Chin. Phys. B* **18** 4177
[30] Zhang B Z, Cui H and She W L 2009 *Chin. Phys. B* **18** 209
[31] Xue J K, Duan W S and Lang H 2002 *Chin. Phys.* **11** 1184
[32] El-Labany S K, Abdel Krim M S, El-Warraki S A and El-Taibany W F 2003 *Chin. Phys.* **12** 759
[33] El-Wakil S A, Abulwafa E M, Elhanbaly A and Abdou M A 2007 *Chaos, Solitons and Fractals* **33** 1512
[34] El-Wakil S A, El-labany S K, Zahran M A and Sabry R 2002 *Phys. Lett. A* **299** 179
[35] Kavitha L, Sathishkumar P and Gopi D 2009 *Phys. Scr.* **79** 015402
[36] Zhu J M 2005 *Chin. Phys.* **14** 1290
[37] He J H 2005 *Chaos, Solitons and Fractals* **26** 695
[38] Zhang J L, Wang Y M, Wang M L and Fang Z D 2003 *Chin. Phys.* **12** 245
[39] He J H 2007 *J. Comput. Appl. Math.* **207** 03
[40] Lin Q, Wu Y H and Loxton R 2009 *J. Phys. A: Math. Theor.* **42** 045207
[41] Yan Z 2003 *J. Phys. A: Math. Gen.* **36** 1961
[42] Kavitha L, Saravanan M, Srividya B and Gopi D 2011 *Phys. Rev. E* **84** 066608
[43] Zhang S 2007 *J. Phys. A: Math. Theor.* **40** 227
[44] Lin X Y and Shi T J 2007 *Chin. Phys.* **16** 310
[45] Malfliet W 1992 *Am. J. Phys.* **60** 650
[46] Malfliet W and Hereman W 1996 *Phys. Scr.* **54** 563
[47] Fan E 2006 *Phys. Lett. A* **277** 212
[48] Yusufoglu E and Bekir A 2008 *Chaos, Solitons and Fractals* **38** 1126
[49] Soliman A A 2006 *Physica A* **361** 394
[50] Kavitha L, Sathishkumar P and Gopi D 2010 *Commun. Nonlinear Sci. Numer. Simul.* **15** 3900
[51] Kavitha L, Prabhu A and Gopi D 2009 *Chaos, Solitons and Fractals* **42** 2322
[52] Kavitha L, Srividya B, Akila N and Gopi D 2010 *Nonlinear Sci. Lett. A* **1** 95
[53] Kavitha L, Srividya B and Gopi D 2010 *J. Magn. Magn. Mater.* **322** 1793
[54] Kavitha L, Akila N, Prabhu A, Kuzmanovska-Barandovska O and Gopi D 2011 *Math. Comput. Modelling* **53** 1095
[55] Kavitha L, Jayanthi S, Muniyappan A and Gopi D 2011 *Phys. Scr.* **84** 035803
[56] Kavitha L, Venkatesh M, Jayanthi S and Gopi D 2012 *Phys. Scr.* **86** 025403
[57] Darvishi M, Najafi M T, Kavitha L and Venkatesh M 2012 *Commun. Theor. Phys.* **58** 785
[58] Wang M L 1995 *Phys. Lett. A* **199** 169
[59] Wang M L 1996 *Phys. Lett. A* **216** 67
[60] Fan E G 2000 *Phys. Lett. A* **265** 353
[61] Peccianti M, Conti C, Assanto A, De Luca D and Umeton C 2002 *Appl. Phys. Lett.* **81** 3335
[62] Henninot J, Debailleul, Asquini R, d'Alessandro A and Warenghem M 2004 *J. Opt. A: Pure Appl. Opt.* **6** 315
[63] Beeckman J, Neyts K, Hutsebaut X and Haelterman M 2006 *Opto-Electronics Rev.* **14** 263
[64] He J H and Wu X H 2006 *Chaos, Solitons and Fractals* **30** 700
[65] He J H 2008 *Int. J. Mod. Phys. B* **22** 3487
[66] He J H 2006 *"Non-perturbative Methods for Strongly Nonlinear Problems"*, Dissertation de-verlag im Internet gmbh, Berlin, Germany
[67] Wu X H and He J H 2007 *Comput. Math. Appl.* **54** 966
[68] Bekir A and Boz A 2007 *Int. J. Nonlinear Sci. Numer. Simul.* **8** 505
[69] Marinakis V 2008 *Z. Naturforsch* **63a** 653
[70] Zhang S and Zhang H Q 2009 *Phys. Lett. A* **373** 2501
[71] Zhu S D 2007 *Int. J. Nonlinear Sci. Numer. Simul.* **8** 461
[72] Zhu S D 2007 *Int. J. Nonlinear Sci. Numer. Simul.* **8** 465
[73] He J H 2012 *Abstract and Applied Analysis* 916793 DOI:10.1155/2012/916793
[74] Kavitha L, Srividya B and Gopi D 2011 *Comput. Math. Appl.* **62** 4691